THE JOURNAL OF PHYSICAL CHEMISTRY B

Article

pubs.acs.org/JPCB

The Influence of Water on the Alkyl Region Structure in Variable Chain Length Imidazolium-Based Ionic Liquid/Water Mixtures

Joseph E. Thomaz, Christian M. Lawler, and Michael D. Fayer*

Department of Chemistry, Stanford University, Stanford, California 94305, United States

ABSTRACT: Solutions of room temperature ionic liquids (RTILs) and water were studied by observing the reorientational dynamics of the fluorescent probe perylene. Perylene is solvated in the alkyl regions of the RTILs. Its D_{2h} symmetry made it possible to extract dynamical information on both in-plane and out-of-plane reorientation from time-resolved fluorescence anisotropy measurements. Perylene reorientation reports on its interactions with the alkyl chains. The RTILs were a series of 1-alkyl-3-methylimidazolium tetrafluoroborates ($C_n$mimBF_4, where n is the number of carbons in the alkyl chain), and the effects on perylene's dynamics were observed when varying the alkyl chain length of the cation (n = 4, 6, 8, and 10; butyl, hexyl, octyl, decyl) and varying the water content from pure RTIL to roughly three water molecules per RTIL ion pair. Time correlated single photon counting was used to measure the fluorescence anisotropy decays to determine the orientational dynamics. The friction coefficients for both the in-plane and out-of-plane reorientation were determined to eliminate the influence of changes in viscosity caused by both the addition of water and the different alkyl chain lengths. The friction coefficients provided information on the interactions of the perylene with the alkyl environment and how these interactions changed with chain length and water content. As the chain length increased, the addition of water had less of an effect on the local alkyl environment surrounding the perylene. The friction coefficients generally increased with higher water contents; the in-plane orientational motion was hindered significantly more than the out-of-plane motion. The restructuring of the alkyl regions is likely a consequence of a rearrangement of the ionic imidazolium head groups to accommodate partial solvation by water, which results in a change in the arrangement of the alkyl chains. At very high water content, $BmimBF_4$ broke this general trend, with both in-plane and out-of-plane rotational friction decreasing above a water content of one water per ion pair. This decrease indicates a major reorganization of the overall liquid structure in high water content mixtures. In contrast to $BmimBF_4$, the longer chain length RTILs are not infinitely miscible with water, and do not show evidence of a major reorganization before reaching saturation and phase-separating. The results suggest that phase separation in longer chain length BF_4 RTILs is a consequence of their inability to undergo the reorganization of the alkyl regions necessary to accommodate high water concentrations.

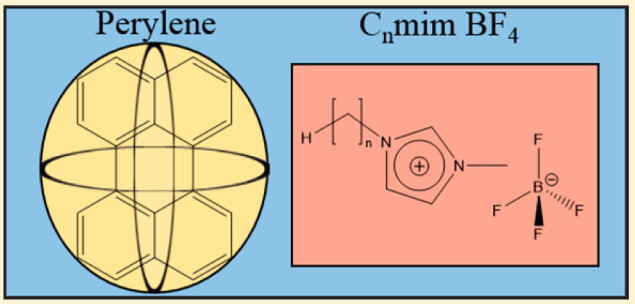

I. INTRODUCTION

Ionic liquids are a class of salt compounds defined as having melting points below 100 °C. If an ionic liquid has a melting point at or below room temperature (25 °C), it is considered to be part of the subclass called room temperature ionic liquids (RTILs). These compounds usually consist of a large asymmetric organic cation paired with a more inorganic anion. The large size and asymmetry of the cations hinder the crystallization of these compounds and give rise to their unusually low melting points.[1,2] RTILs have much lower vapor pressures than more traditional organic solvents, making them the object of study for use in a wide range of applications such as batteries,[3−5] separations,[6,7] and solvents in chemical synthesis.[8−10]

The mesoscopic structure of ionic liquids has been the subject of significant interest.[11−14] The concept of nanoscopic heterogeneity in RTILs first arose in molecular dynamics simulations where it was observed that alkyl tails would aggregate, forming organic regions isolated from the cationic head groups and anions.[11,13] Since then, this model has generated meaningful interpretations of data acquired in a variety of different experiments such as small-angle X-ray scattering (SAXS),[15] small-angle neutron scattering (SANS),[16] NMR,[17,18] dielectric spectroscopy,[19,20] optically heterodyne detected optical Kerr effect (OHD-OKE),[21−25] time-resolved fluorescence,[21,26−28] and 2D infrared spectroscopy (2D IR).[29−31] These simulations also demonstrated that RTILs with longer alkyl chains had more well-defined apolar regions with larger organic domains.[32]

Understanding the effect that water has on the bulk structure of ionic liquids is important because of their inherently hygroscopic nature.[33] As a result of this high affinity for water, commercially purchased RTILs typically contain non-negligible amounts of it. The effects of water on RTIL properties become evident even in miniscule quantities;[9,34,35] a water contamination on the order of 0.015 mole fraction in 1-

Received: August 3, 2016
Revised: September 16, 2016
Published: September 19, 2016

DOI: 10.1021/acs.jpcb.6b07853
J. Phys. Chem. B 2016, 120, 10350−10357

decyl-3-methylimidazolium tetrafluoroborate reduces its bulk viscosity by 28% compared to the neat liquid.[22] Water/RTIL mixtures are the subject of research for catalytic reactions in which water is intentionally used as cosolvent.[36] Additionally, due to their high conductivities and low volatility, these mixtures have also been considered as solvents for swelling proton exchange membranes such as Nafion commonly used in fuel cells.[37]

In this study, time correlated single photon counting (TCSPC) orientational anisotropy experiments were conducted using perylene as a fluorescent probe of the organic regions of a series of 1-alkyl-3-methylimidazolium tetrafluoroborate ($[C_n mim][BF_4]$) RTILs with n = 4, 6, 8, and 10, Bmim, Hmim, Omim, and Dmim, respectively (see Figure 1). Water

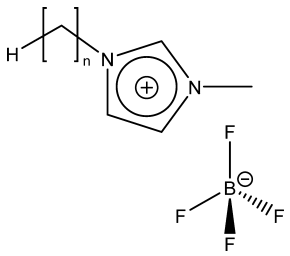

Figure 1. Structure of 1-alkyl-3-methylimidizolium tetrafluoroborate expressed as $C_n mimBF_4$, where n refers to the length of the alkyl chain. n = 4, 6, 8, 10.

content in the RTILs was varied from dry to ~0.75 mole fraction water as the saturation point of each RTIL permitted. The fluorescent hydrocarbon perylene was selected to probe the nonpolar alkyl regions of the BF_4 RTILs because its D_{2h} symmetry (see Figure 2) permits substantial information regarding its orientational dynamics to be obtained from fluorescence anisotropy experiments.

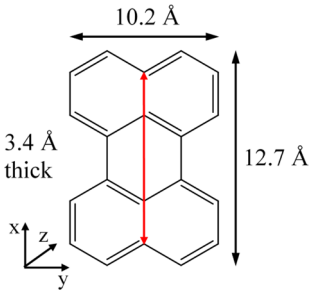

Figure 2. Structure and dimensions of perylene. Rotation about the z-axis is in-plane; rotation about the y-axis is out-of-plane. The transition dipole direction, shown in red, lies along the x-axis.

Detailed studies to determine the location of aromatic compounds within alkylimidazolium-based RTIL solutions have been previously conducted.[38] Through NMR studies, it was found that single ring aromatic compounds may lie in the ionic region as a result of π-stacking interactions.[39,40] In contrast, this was not found to be true in larger polyaromatic compounds.[26] In addition, a study conducted on perylene in an alkylimidazolium-based RTIL demonstrated that, as chain length increases, the perylene approaches an environment akin to that of a mineral oil, further supporting the notion that the dynamics of perylene report on the organic domains.[21]

Perylene's $S_1 \rightarrow S_0$ emission transition dipole lies on the long-axis in the coordinate system shown in Figure 2 (red arrow).[41] Because perylene has such high symmetry and the alignment of its transition dipole is along a molecular axis, it is possible to extract both the in-plane and out-of-plane orientational relaxation dynamics from its time-dependent fluorescence anisotropy.[42] Using the anisotropy data, the perylene friction coefficients are determined as a function of water content and alkyl chain length. The friction coefficients provide information on the nature of the orientational relaxation independent of the changes in viscosity, which accompany changes in water content and alkyl chain length.

OHD-OKE experiments have previously been conducted on $C_n mimBF_4$ ionic liquids with varying water contents ranging from the pure ionic liquid to ~0.75 mole fraction water, the concentration at which longer chained ionic liquids become water-saturated. It was found that long chained BF_4 RTILs ($OmimBF_4$ and $DmimBF_4$) yielded longer than expected anisotropy decays. The slow orientational relaxation was attributed to a stiffening of the tail−tail interactions in the alkyl region.[22] It is of considerable interest to study the organic regions directly; the OHD-OKE study mainly reported on the behavior of the cationic imidazolium head group. Here we report on the alkyl region's response to reorganization of the ionic region as water is added by examining the trends in the friction coefficients. It was found that the alkyl chain length has a substantial impact on the organic region structure as water is added to the ionic domains. The longest chain length studied, n = 10, shows little evidence of reorganization of the alkyl region structure upon the addition of water. However, as the chain length becomes shorter, the extent of alkyl region restructuring with water addition increases. At high water content, all of the liquids (n = 10, 8, and 6) phase separate except for $BmimBF_4$ (n = 4). In the water content range where the longer chain RTILs approach phase separation, the $BmimBF_4$ friction coefficient trend deviates markedly from that of its longer chained analogues.

II. MATERIALS AND METHODS

The $C_n mimBF_4$ RTILs were purchased from IoLiTec at 99% HP grade and were subsequently placed in a vacuum and dried for 1 week at a temperature of 60 °C. Water content in each of the ionic liquids was measured to be under 30 ppm using Karl Fischer titration. A stock solution of perylene in methylene chloride was made. When preparing an ionic liquid sample, an appropriate amount of stock solution was placed in the bottom of a scintillation vial such that the final perylene concentration in ionic liquid would be 10^{-5} M and the solvent was evaporated. The vial was then put into a glovebox where the ionic liquid was added to the scintillation vial along with a stir bar, and the perylene/RTIL solution was stirred. The addition of water, when necessary, was performed by using a micropipette to deposit the desired amount of water into a perylene/RTIL mixture and the solution was sonicated for 30 min.

The time correlated single photon counting (TCSPC) technique was used to conduct the fluorescence anisotropy experiments. The excitation source was a Ti:sapphire oscillator, which produced ~100 fs laser pulses at a wavelength of 790 nm. This wavelength was frequency doubled in a barium borate crystal to 395 nm for excitation of perylene. The bandwidth of the 395 nm excitation pulses was 5.8 nm. An acousto-optic modulator was used as a single pulse selector to reduce the laser

DOI: 10.1021/acs.jpcb.6b07853
J. Phys. Chem. B 2016, 120, 10350−10357

repetition rate from 80 to 5 MHz. A half wave plate mounted in a computer controlled rotator was used to rotate the polarization of the excitation beam relative to a fixed polarizer mounted on the entrance slit of a monochromator. The sample was excited from the front surface in an essentially normal geometry through a hole in the lens that collected the fluorescence. A second lens imaged the fluorescence onto the monochromator entrance slit. The collected fluorescence was frequency resolved by the monochromator, and single photons were detected with a multichannel plate detector (MCP) at a wavelength of 440 nm.

The instrument response was obtained by measuring the fluorescence lifetime of aqueous acidified malachite green with an optical density matching that of the sample, under identical experimental conditions to the sample measurements. Malachite green has an extremely short fluorescence lifetime, 5 ps, which is short compared to the instrument response,[28] so a measurement of its fluorescence lifetime on this system gives the instrument response including the effects of the finite thickness of the sample cell. The instrument response was found to be no more than 85 ps fwhm.

It is common for $C_n$mimBF_4 RTILs to be contaminated with fluorescent impurities. It has been documented that these contaminants are generally negligible in concentration, do not have a significant effect on the bulk structure of the ionic liquid, and only become apparent with techniques such as fluorescence.[43,44] Such contaminants are excited at the 395 nm sample excitation wavelength and emit at 440 nm, meaning that when present they contribute to the experimental fluorescent decays. Because of the very low concentration of both the perylene and the impurities, it is a safe assumption that they will not interact with each other when solvated by ionic liquids. The contributions of the perylene and the contaminants to the fluorescence decays are therefore additive. For this reason, data from reference samples containing only the RTIL/water mixtures with no dissolved probe were also collected. A moving sample stage was used that interchanges the two samples under computer control so that data were collected on both the ionic liquid samples, alternating between those with perylene and those without, keeping all experimental conditions identical over the course of the experiment. The resulting perylene lifetime decay curves attained after subtraction of the reference sample fluorescence decay were single exponentials with time constants of 5.02 ns within experimental error for all RTILs studied. The measured lifetime is consistent with the perylene lifetime in other solvents.[45] This observed single exponential decays with the same lifetimes indicates the reliability of the background subtraction technique for removing the contribution of fluorescent impurities in the RTILs. Because of the absence of fluorescent impurities, Hmim BF_4 samples did not require subtraction, and it yielded the same fluorescent lifetime, within error, as the other samples. Furthermore, two different batches of Bmim BF_4 from the supplier were used in the Bmim experiments. One batch had fluorescence impurities and required the impurity fluorescence subtraction. No subtraction was performed on the batch without impurities. The results obtained from both batches were the same, clearly demonstrating the validity of the background subtraction method.

III. RESULTS AND DISCUSSION

The time-dependent fluorescence anisotropy of the perylene probe was measured to obtain information on its orientational dynamics. Fluorescence anisotropy is measured by collecting fluorescence intensity decays with polarization parallel, $I_{\parallel}(t)$, and perpendicular, $I_{\perp}(t)$, to the excitation polarization. These decays are given by

$$I_{\parallel}(t) = P(t)(1 + 0.8C_2(t)) \tag{1}$$

$$I_{\perp}(t) = P(t)(1 - 0.4C_2(t)) \tag{2}$$

$P(t)$ is the excited state population decay, and $C_2(t)$ is the second order Legendre polynomial orientational correlation function. $P(t)$ and $C_2(t)$ are expressed as functions of $I_{\parallel}(t)$ and $I_{\perp}(t)$ and show the relationship between $C_2(t)$ and the fluorescence anisotropy $r(t)$.

$$r(t) = \frac{I_{\parallel}(t) - I_{\perp}}{I_{\parallel}(t) + 2I_{\perp}} \tag{3}$$

$$P(t) = \frac{1}{3}(I_{\parallel}(t) + 2I_{\perp}(t)) \tag{4}$$

with

$$r(t) = 0.4C_2(t) \tag{5}$$

Therefore, $r(t)$ reports solely on orientational relaxation with the population decay removed.

Figure 3 shows time dependent anisotropy decays, $r(t)$, of perylene in HmimBF_4 samples with different water contents. Similar plots were generated for each RTIL chain length. It was determined that the data fit well to multiexponential decays across all levels of hydration. Fits to all data began at 200 ps to eliminate the need for convolutions with the instrument response. The inset in Figure 3 shows the HmimBF_4 4:1 data (magenta curve) and a biexponential fit (black dashed curve). The time constants for each fit as well as the bulk viscosity of each solution are given in Table 1. From the table, it is evident that the reorientation times of the perylene decrease with increasing water content, which decreases the bulk viscosity of the RTIL. The decreasing viscosity is a significant contributor to the decreasing reorientational time of perylene. To study the system further, it becomes necessary to use a viscosity independent measure. For this purpose, the in-plane and out-of-plane rotational friction coefficients were calculated for perylene in each RTIL/water solution.

To obtain the friction coefficients, first rotational diffusion constants must be extracted from the anisotropy data. Equation 6 gives the anisotropy decay for the general case of orientational diffusion of a molecule undergoing diffusive orientational relaxation

$$\begin{aligned} r(t) = \frac{6}{5}(&q_y q_z \gamma_y \gamma_z e^{-3(D_x+D)t} + q_x q_z \gamma_x \gamma_z e^{-3(D_y+D)t} \\ &+ q_x q_y \gamma_x \gamma_y e^{-3(D_z+D)t}) + \frac{3}{10}((\alpha+\beta)e^{-(6D+2\Delta)t} \\ &+ (\alpha-\beta)e^{-(6D-2\Delta)t}) \end{aligned} \tag{6}$$

where

$$\begin{aligned} \alpha = \frac{1}{\Delta}[&D_x(q_y^2\gamma_y^2 + q_z^2\gamma_z^2 - 2q_x^2\gamma_x^2 + q_x^2 + \gamma_x^2) \\ &+ D_y(q_x^2\gamma_x^2 + q_z^2\gamma_z^2 - 2q_y^2\gamma_y^2 + q_y^2 + \gamma_y^2) \\ &+ D_z(q_x^2\gamma_x^2 + q_y^2\gamma_y^2 - 2q_z^2\gamma_z^2 + q_z^2 + \gamma_z^2) - 2D] \end{aligned} \tag{7}$$

DOI: 10.1021/acs.jpcb.6b07853
J. Phys. Chem. B 2016, 120, 10350−10357

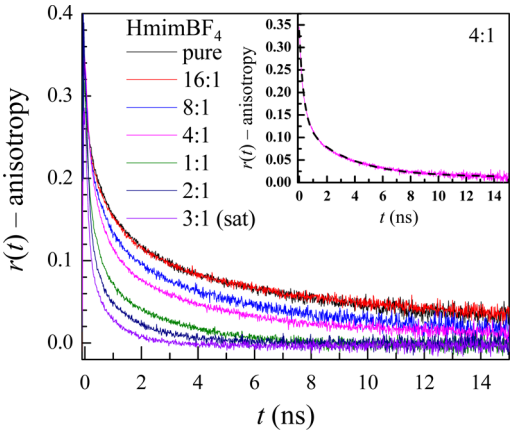

Figure 3. Time-dependent anisotropy decays, $r(t)$, for $HmimBF_4$ with varying water content from pure $HmimBF_4$ (no water added) to the saturation point at which it phase separates. Water content ratios in the legend are expressed as $HmimBF_4$ ion pairs:H_2O. The inset shows the 4:1 data (magenta curve) with a biexponential fit to the data (black dashed curve).

Table 1. Viscosities and Anisotropy Time Constants for $HmimBF_4$ as a Function of Water Content

$HmimBF_4$:H_2O[a]	η[b] (cP)	τ_1[c] (ns)	τ_2[c] (ns)
pure	190	0.74	6.08
16:1	145	0.83	6.00
8:1	112	0.66	5.18
4:1	76.6	0.46	4.23
1:1	23.8	0.27	2.23
2:1	12.7	0.24	1.51
3:1	8.98	0.24	1.29

[a]Mol ratio of $HmimBF_4$:H_2O. Pure has <30 ppm of H_2O. [b]Dynamic viscosities measured with a rotary viscometer; error bars ≤1%. [c]Time constants from biexponential fits to the anisotropy decays; error bars given in Table 2.

$$\beta = q_x^2\gamma_x^2 + q_y^2\gamma_y^2 + q_z^2\gamma_z^2 - \frac{1}{3} \tag{8}$$

$$D = \frac{1}{3}(D_x + D_y + D_z) \tag{9}$$

$$\Delta = \sqrt{D_x^2 + D_y^2 + D_z^2 - D_xD_y - D_xD_z - D_yD_z} \tag{10}$$

Equation 6 is a sum of five exponentials where q_i and γ_i are the projections of the excitation and emission dipoles onto the ith molecular axis and D_i is the orientational diffusion constant for rotation about that same axis i.[46]

Because perylene's absorption and emission transition dipoles lie along the long molecular axis (the x axis in the axis system of Figure 1), rotation about this axis does not cause fluorescence depolarization, and the diffusion constant D_x cannot be determined from fluorescence anisotropy measurements. Equation 6 can be simplified greatly by modeling perylene as an oblate spheroid, for which $D_x = D_y \ll D_z$, where D_y is the out-of-plane orientational diffusion constant and D_z is the in-plane orientational diffusion constant. This treatment, which has been used and validated in previous work on perylene in imidazolium-based RTILs,[21,27] results in a biexponential expression for the anisotropy of the form

$$r(t) = A_1 e^{-(2D_y+4D_z)t} + A_2 e^{-6D_y t} \tag{11}$$

$r(0)$ for perylene is consistently less than the predicted value of 0.4, as a result of ultrafast inertial orientational relaxation.[47] Table 2 lists the time constants and their associated in-plane and out-of-plane diffusion coefficients for perylene in each RTIL/water solution.

It is notable that for low water content anisotropies in long chained RTILs ($OmimBF_4$ and $DmimBF_4$) the decays are triexponential rather than biexponential as hydrodynamic theory predicts. Orientational probes in solution can have fast limited-range motions, which may be inertial or diffusive.[47−49] We propose that the fastest decay in the most viscous solutions reflects a fast, limited-range "wobbling-in-a-cone"[50,51] motion of perylene. At short time, perylene can sample a limited range of angles, the cone. At longer times, local constraints are released and the perylene can undergo full orientational diffusion, sampling all angles. In lower viscosity RTIL/water mixtures, this motion is likely still present but is too fast to observe given the time resolution of the instrumentation. Because we are interested in the probe's rotational diffusion leading to complete orientational randomization, for the water/RTIL mixtures in which a triexponential anisotropy decay was observed, we examine only the two slower time constants that determine the in-plane and out-of-plane orientational diffusion constants.

Previous studies have rigorously demonstrated that perylene orientational relaxation behaves hydrodynamically in ionic liquids;[21,27] that is, the Debye−Stokes−Einstein (DSE) relationship can be used to relate the diffusion constant to the viscosity and the temperature. The fact that perylene in ionic liquids obeys the DSE equation makes it possible to obtain friction coefficients. When water is added, the bulk viscosity decreases. Examining the water concentration and chain length dependences of the friction coefficients permits the influence of changing viscosity to be removed. Then, it is possible to address whether there are changes in orientational dynamics caused by changes in liquid structure independently from changes in viscosity. The friction coefficient for rotation about the ith axis is

$$\lambda_i = \frac{kT}{\eta V D_i} \tag{12}$$

where η is the viscosity, T is the temperature (24.5 °C), and V is the molecular volume of the probe (225 Å^3 for perylene[21]).

Friction coefficients are used to extract the effects of changing water concentration on the probe's orientational dynamics, independent of viscosity and temperature. These values are then compared to theoretical literature values for an ellipsoid of the same dimensions. Perylene is smaller or of comparable size to the ionic liquid solvent without strong interactions with the solvent, such as hydrogen bonding, making slip boundary conditions appropriate for the analysis. For slip boundary conditions, the resistance to the rotation of a solute arises from displacement of solvent within its swept volume. Stick boundary conditions are in contrast to slip boundary conditions in which the molecular probe is substantially larger than the solvent and drags solvent molecules along as it rotates.

For an ellipsoid with axes matching the molecular dimension of perylene, the theoretical slip rotational friction coefficients are 7.03 for the out-of-plane rotation and 0.37 for in-plane rotation.[52,53] Here, we present experimental friction coefficients normalized to the theoretical hydrodynamic slip boundary

DOI: 10.1021/acs.jpcb.6b07853
J. Phys. Chem. B 2016, 120, 10350−10357

Table 2. Chain Length and Water Concentration Dependent Viscosities, Anisotropy Decay Constants, Orientational Diffusion Constants, and Friction Coefficient Ratios

RTIL:H_2O[a]	η[b] (cP)	τ_1[c] (ns)	τ_2[c] (ns)	τ_3[c] (ns)	D_z[d] (ns^{-1})	D_y[d] (ns^{-1})	λ_z[e] ratio	λ_y[e] ratio
				BmimBF$_4$				
pure	103		0.69 ± 0.03	4.11 ± 0.1	0.34 ± 0.04	0.041 ± 0.003	1.56 ± 0.20	0.58 ± 0.05
14:1	76.2		0.64 ± 0.05	4.08 ± 0.2	0.37 ± 0.03	0.041 ± 0.007	1.94 ± 0.22	0.78 ± 0.14
3:1	36.7		0.44 ± 0.05	2.82 ± 0.2	0.54 ± 0.04	0.059 ± 0.010	2.76 ± 0.29	1.12 ± 0.19
1:1	14		0.31 ± 0.01	1.75 ± 0.04	0.76 ± 0.06	0.095 ± 0.016	5.13 ± 0.53	1.82 ± 0.31
1:2	8.5		0.15 ± 0.06	0.67 ± 0.05	1.53 ± 0.25	0.25 ± 0.015	4.20 ± 0.69	1.15 ± 0.07
1:3	6.46		0.11 ± 0.05	0.50 ± 0.06	2.06 ± 0.24	0.33 ± 0.015	4.10 ± 0.48	1.13 ± 0.05
				HmimBF$_4$				
pure	190		0.74 ± 0.02	6.08 ± 0.03	0.24 ± 0.03	0.025 ± 0.008	1.2 ± 0.17	0.5 ± 0.15
16:1	145		0.83 ± 0.03	6.00 ± 0.2	0.29 ± 0.04	0.028 ± 0.010	1.32 ± 0.20	0.6 ± 0.21
8:1	112		0.66 ± 0.03	5.18 ± 0.2	0.36 ± 0.06	0.032 ± 0.010	1.35 ± 0.21	0.67 ± 0.20
4:1	76.6		0.46 ± 0.02	4.23 ± 0.07	0.52 ± 0.08	0.039 ± 0.005	1.36 ± 0.21	0.8 ± 0.10
1:1	23.8		0.27 ± 0.004	2.23 ± 0.06	0.89 ± 0.07	0.075 ± 0.008	2.58 ± 0.21	1.36 ± 0.14
1:2	12.7		0.24 ± 0.005	1.51 ± 0.02	0.98 ± 0.05	0.11 ± 0.004	4.38 ± 0.21	1.73 ± 0.06
1:3	8.98		0.24 ± 0.02	1.29 ± 0.03	0.96 ± 0.08	0.13 ± 0.006	6.34 ± 0.5	2.03 ± 0.09
				OmimBF$_4$				
pure	352	0.23 ± 0.05	1.29 ± 0.04	10.5 ± 0.2	0.19 ± 0.04	0.016 ± 0.004	1.17 ± 0.24	0.54 ± 0.15
14:1	243		0.82 ± 0.06	8.22 ± 0.3	0.30 ± 0.09	0.020 ± 0.008	0.75 ± 0.23	0.49 ± 0.27
6:1	174		0.55 ± 0.05	5.48 ± 0.4	0.44 ± 0.04	0.030 ± 0.002	0.72 ± 0.07	0.46 ± 0.07
3:1	116		0.39 ± 0.05	3.72 ± 0.1	0.63 ± 0.15	0.044 ± 0.010	0.75 ± 0.18	0.47 ± 0.10
1:1	54.9		0.30 ± 0.05	2.73 ± 0.1	0.80 ± 0.15	0.061 ± 0.020	1.24 ± 0.23	0.72 ± 0.22
1:2.5	24.2		0.24 ± 0.04	2.06 ± 0.1	0.99 ± 0.10	0.080 ± 0.021	2.28 ± 0.52	1.24 ± 0.32
				DmimBF$_4$				
pure	630	0.45 ± 0.04	1.99 ± 0.15	16.16 ± 0.4	0.10 ± 0.08	0.010 ± 0.007	0.87 ± 0.68	0.38 ± 0.25
64:1	452	0.35 ± 0.03	1.99 ± 0.15	16.2 ± 0.4	0.10 ± 0.02	0.010 ± 0.007	1.23 ± 0.23	0.53 ± 0.36
13:1	376	0.14 ± 0.03	1.62 ± 0.05	12.6 ± 0.3	0.15 ± 0.001	0.013 ± 0.006	0.98 ± 0.08	0.48 ± 0.23
6:1	294		0.51 ± 0.03	5.85 ± 0.2	0.48 ± 0.19	0.029 ± 0.007	0.39 ± 0.23	0.29 ± 0.07
3:1	203		0.42 ± 0.08	3.96 ± 0.3	0.58 ± 0.18	0.042 ± 0.019	0.46 ± 0.23	0.28 ± 0.13
1:1	96		0.37 ± 0.04	3.11 ± 0.2	0.65 ± 0.14	0.053 ± 0.015	0.88 ± 0.19	0.47 ± 0.13
1:2.35	57.5		0.246 ± 0.07	1.95 ± 0.2	0.97 ± 0.08	0.086 ± 0.015	0.43 ± 0.19	0.29 ± 0.05

[a]Mol ratio of RTIL ion pair:H_2O. Concentrations labeled "pure" were determined to be <30 ppm of H_2O. [b]Dynamic viscosity measured with a rotary viscometer; error bars were found to be ≤1%. [c]Time constants extracted from multiexponential fits of anisotropy decays. [d]In-plane and out-of-plane rotational diffusion coefficients respectively extracted from anisotropy fits. [e]In-plane and out-of-plane friction coefficient ratios respectively extracted using eq 12 and normalized to the slip boundary condition theoretical values of 0.37 for in-plane and 7.03 for out-of-plane.

condition values to better emphasize the effect of the solvent environment on the rotation of the probe; without normalizing to the theoretical values, the out-of-plane friction coefficient is much larger than the in-plane coefficient because the out-of-plane rotation requires displacing a much greater volume of solvent. If the rotation is perfectly hydrodynamic and the only effect of changing water concentration on perylene's solvent environment is the reduction of the bulk viscosity, the normalized friction coefficients will be constant and equal to 1. However, if the perylene interactions with the solvent change with sample composition because of reorganization of the liquid structure changing the solvent interactions with the perylene probe, the normalized friction coefficients will change.

The friction coefficient ratios using slip boundary conditions across all ionic liquid chain lengths and water contents were computed and are shown in Figure 4 for the in-plane and out-of-plane components. Figure 4A shows out-of-plane friction coefficients as a function of the mole fraction of water, while Figure 4B shows the in-plane counterpart. For the pure liquids (no water added), the in-plane values are close to 1, which, for the out-of-plane component, the pure values are close to 0.5.

As chain length increases, there is a decrease in variation of the friction coefficients with water content to the point where there is no substantial change in the friction coefficients of DmimBF$_4$ over the entire range of water contents. In all the shorter-chain RTILs, however, the change in friction coefficients with water concentration shows that the orientational dynamics of perylene do not simply track the bulk viscosity of the liquid, indicating structural changes in the local liquid environment of perylene. Previous studies have shown that, with increasing chain size, the organic regions of the RTILs become both larger and more clearly segregated from the ionic region.[14,32] Water molecules located in the ionic regions make hydrogen bonds to the anions. Addition of water will cause the structure of the ionic region to change, which in turn can impact the arrangement of the alkyl chains. The results displayed in Figure 4 show that changes in the structure of the ionic regions with the addition of water have a decreasing effect as the alkyl chain length gets longer. For Dmim with its 10-carbon chain, there is little or no change in the alkyl region structure induced by the addition of water. For Hmim, with its 6-carbon chain, there is a substantial change in friction, demonstrating a substantial change in the alkyl chain arrangement. Bmim (4 carbons) has an even steeper dependence on the water content to a mole fraction of 0.5; then, the trend reverses directions. This difference between Bmim and the other RTILs is discussed below.

DOI: 10.1021/acs.jpcb.6b07853
J. Phys. Chem. B 2016, 120, 10350−10357

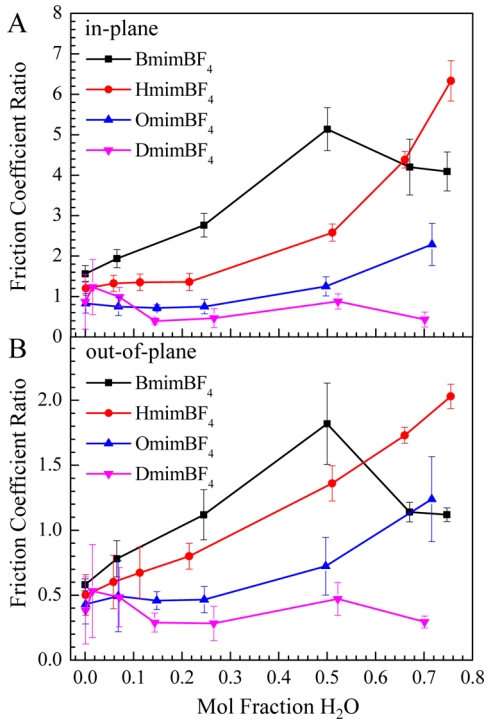

Figure 4. Friction coefficient ratios plotted against the mole fraction of H_2O for all RTILs. The friction coefficients, extracted using eq 12, were normalized to the slip boundary condition theoretical values of 0.37 for in-plane friction in part A and 7.03 for out-of-plane friction in part B.

With the exception of $DmimBF_4$, where there is little difference, in-plane friction coefficients show a somewhat larger change with increasing water content than their out-of-plane equivalents. For example, the in-plane normalized coefficient for Hmim goes from 1.2 to 6.3, while the out-of-plane coefficient goes from 0.5 to 2. The changes in the in-plane friction coefficient result from impedance of motion on the perimeter of the molecular probe, while changes in the out-of-plane friction coefficient result from impedance of motion over the surface area of the molecular probe. The results indicate that the increase in water content changes the alkyl region structure in such a way that the perylene experiences hindrance to its reorientation to a greater degree at the perimeter (in-plane) while having less of an effect on the out-of-plane sweeping motion.

The most conspicuous result in both plots is the sudden drop in friction coefficient on the Bmim trace between 0.5 and 0.75 mole fraction water. Adding water to the ionic regions promotes rearrangement of the anions and cationic head groups to accommodate the partial solvation. A study conducted by Raos and co-workers found that at low water content $BmimBF_4$, RTIL ions coordinate with the water molecules; as water content increases, water clusters are formed within the ionic domains of the RTIL.[54] However, rearrangement of the ions requires changes of the structure in the organic regions, which becomes more difficult as the chain length increases.[1] For $Dmim^+$, addition of water makes little change in the organic region. The changes increase as the chain lengths decrease, with $Bmim^+$ showing the largest change. For $Bmim^+$ at the highest water concentration, the alkyl chains do not prevent a major rearrangement of the ionic regions, which in turn produces a large change in the structure of the alkyl regions. This change is not seen in the other RTILs because the reorganization of the ionic domains is not capable of forcing the longer alkyl tails to restructure. Simulations by Voth and co-workers suggest a local structure change near 0.75 mole fraction water in the organic region of BF_4 RTILs in which there is a breakdown of the alkyl region in $Bmim^+$ not observed for longer chain lengths.[55] $BmimBF_4$ is completely miscible with water, while the longer chain length RTILs undergo phase separation at ~0.7 mole fraction. The inability of the longer chain (≥6) RTILs to accommodate large scale reorganization of the ionic regions at high water content because of the price paid for the required restructuring of the alkyl region may be the cause of the phase separation observed between 0.7 and 0.75 mole fraction water in the longer chain BF_4 RTILs. In contrast, $BmimBF_4$ is miscible with water. The water content dependent friction coefficients for this molecule show evidence of a major reorganization of the alkyl region in the range of water concentrations where phase separation occurs with longer chain RTILs.

The systems C_nmimBF_4 as a function of water concentration were studied previously using optical heterodyne detected optical Kerr (OHD-OKE) effect measurements.[22] OHD-OKE experiments measure the orientational relaxation dynamics of the bulk liquid. The data decay as two power laws at short time followed by a final exponential decay. The power laws reflect nondiffusive orientational relaxation caused by "caging", and the exponential is the final diffusive complete orientational relaxation of the liquid. This general form has been seen in many liquids[56,57] and is consistent with analysis of supercooled liquids using schematic mode coupling theory (MCT).[58]

As water was added to $BmimBF_4$, the final exponential decay became fast in a manner consistent with hydrodynamic behavior; that is, the orientational relaxation time constants vs viscosity fell on a line.[22] However, $DmimBF_4$ behaved in a very different manner. At higher water concentrations, the longtime decay was nonexponential. The decay is an exponential to essentially an offset followed by a much slower final exponential decay. These data were interpreted as a wobbling-in-a-cone of the imidazolium head group (the faster exponential decay) followed by the final complete orientational relaxation. $BmimBF_4$ did not display this behavior. It was argued that the long alkyl chains of $DmimBF_4$ greatly impeded the bulk liquids orientation relaxation, giving rise to the observation of the wobbling and the nonhydrodynamic final orientational relaxation.[22] The current results are in accord with and compliment the OHD-OKE studies.

IV. CONCLUDING REMARKS

Time correlated single photon counting experiments were performed on perylene to collect fluorescence lifetime and orientational anisotropy decays on a series of C_nmimBF_4 RTILs with varying water content from no water to roughly 0.75 mole fraction water. RTIL/water mixtures without perylene were used as reference samples to remove fluorescent contributions from low concentration contaminants found in commercial RTILs. Excited state lifetime decays showed that there is a single population of perylene molecules in all RTIL/water mixtures allowing orientational diffusion constants D_i to be extracted from the anisotropy decays. Using the Debye–Stokes–Einstein relation, the in-plane and out-of-plane friction coefficients, λ_i, were calculated from the orientational diffusion constants.

DOI: 10.1021/acs.jpcb.6b07853
J. Phys. Chem. B 2016, 120, 10350–10357

In long chain RTIL, $DmimBF_4$, increasing water content had no significant effect on the in-plane and out-of-plane friction coefficients (Figure 4). Changes of structure in the ionic regions caused by water solvation of the ions are insufficient to reorganize the alkyl regions because of the substantial favorable interactions among the long chains. As the chain length was decreased, however, the addition of water caused both friction coefficients to increase, with the increases becoming larger as the chain length became shorter. It was observed that in-plane friction coefficients were affected more than their out-of-plane analogues.

For $BmimBF_4$ (n = 4), the trend of a monotonically increasing friction coefficient with increasing water content was reversed at high water contents, over 0.5 mole fraction water. The longer chain RTILs phase separate at a water content of ~0.7 mole fraction, but $BmimBF_4$ is completely miscible with water. The nonmonotonic behavior of the $BmimBF_4$ friction coefficients (Figure 4) may indicate the ability of the alkyl regions to sustain large changes in structure to accommodate favorable solvation structures in the ionic regions. The longer alkyl chains resist major structural rearrangements that would accompany favorable solvation structures in the ionic regions. The result is phase separation rather than major changes in the alkyl region structure.

AUTHOR INFORMATION

Corresponding Author

*E-mail: fayer@stanford.edu. Phone: (650) 723-4446.

Notes

The authors declare no competing financial interest.

ACKNOWLEDGMENTS

This work was funded by the Division of Chemical Sciences, Geosciences, and Biosciences, Office of Basic Energy Sciences of the U.S. Department of Energy through Grant No. DE-FG03-84ER13251 (C.M.L. and M.D.F.) and by the Division of Chemistry, Directorate of Mathematical and Physical Sciences, National Science Foundation (NSF) (CHE-1461477) (J.E.T. and M.D.F.). J.E.T. thanks the NSF for a graduate research fellowship.

REFERENCES

(1) Hayes, R.; Warr, G. G.; Atkin, R. Structure and Nanostructure in Ionic Liquids. *Chem. Rev.* **2015**, *115*, 6357−6426.

(2) Plechkova, N. V.; Seddon, K. R. Applications of Ionic Liquids in the Chemical Industry. *Chem. Soc. Rev.* **2008**, *37*, 123−150.

(3) Howlett, P. C.; Brack, N.; Hollenkamp, A. F.; Forsyth, M.; Macfarlane, D. R. Characterization of the Lithium Surface in N-Methyl-N-Alkylpyrrolidinium Bis(Trifluoromethanesulfonyl)Amide Room-Temperature Ionic Liquid Electrolytes. *J. Electrochem. Soc.* **2006**, *153*, A595−A606.

(4) Xue, L.; Tucker, T. G.; Angell, C. A. Ionic Liquid Redox Catholyte for High Energy Efficiency, Low-Cost Energy Storage. *Adv. Energy Mater.* **2015**, *5*, 1500271.

(5) Lin, M.-C.; Gong, M.; Lu, B.; Wu, Y.; Wang, D.-Y.; Guan, M.; Angell, M.; Chen, C.; Yang, J.; Hwang, B.-J.; Dai, H. An Ultrafast Rechargeable Aluminium-Ion Battery. *Nature* **2015**, *520*, 324.

(6) Han, X.; Armstrong, D. W. Ionic Liquids in Separations. *Acc. Chem. Res.* **2007**, *40*, 1079−1086.

(7) Kohno, Y.; Ohno, H. Ionic Liquid/Water Mixtures: From Hostility to Conciliation. *Chem. Commun.* **2012**, *48*, 7119−7130.

(8) Welton, T. Room-Temperature Ionic Liquids. Solvents for Synthesis and Catalysis. *Chem. Rev.* **1999**, *99*, 2071−2083.

(9) Khupse, N. D.; Kumar, A. The Cosolvent-Directed Diels-Alder Reaction in Ionic Liquids. *J. Phys. Chem. A* **2011**, *115*, 10211−10217.

(10) Kubisa, P. Ionic Liquids in the Synthesis and Modification of Polymers. *J. Polym. Sci., Part A: Polym. Chem.* **2005**, *43*, 4675−4683.

(11) Wang, Y.; Voth, G. A. Unique Spatial Heterogeneity in Ionic Liquids. *J. Am. Chem. Soc.* **2005**, *127*, 12192−12193.

(12) Margulis, C. J. Computational Study of Imidazolium-Based Ionic Solvents with Alkyl Substituents of Different Lengths. *Mol. Phys.* **2004**, *102*, 829−838.

(13) Canongia Lopes, J. N. A.; Padua, A. A. H. Nanostructural Organization in Ionic Liquids. *J. Phys. Chem. B* **2006**, *110*, 3330−3335.

(14) Triolo, A.; Russina, O.; Bleif, H.-J.; Di Cola, E. Nanoscale Segregation in Room Temperature Ionic Liquids. *J. Phys. Chem. B* **2007**, *111*, 4641−4644.

(15) Russina, O.; Triolo, A.; Gontrani, L.; Caminiti, R.; Xiao, D.; Hines, L. G. J.; Bartsch, R. A.; Quitevis, E. L.; Pleckhova, N.; Seddon, K. R. Morphology and Intermolecular Dynamics of 1- Alkyl-3-Methylimidazolium Bis(Trifluoromethane)Sulfonylamide Ionic Liquids: Structural and Dynamic Evidence of Nanoscale Segregation. *J. Phys.: Condens. Matter* **2009**, *21*, 424121.

(16) Atkin, R.; Warr, G. G. The Smallest Amphiphiles: Nanostructure in Protic Room-Temperature Ionic Liquids with Short Alkyl Groups. *J. Phys. Chem. B* **2008**, *112*, 4164−4166.

(17) Chiappe, C. Nanostructural Organization of Ionic Liquids: Theoretical and Experimental Evidences of the Presence of Well Defined Local Structures in Ionic Liquids. *Monatsh. Chem.* **2007**, *138*, 1035−1043.

(18) Imanari, M.; Uchida, K. I.; Miyano, K.; Seki, H.; Nishikawa, K. NMR Study on Relationships between Reorientational Dynamics and Phase Behaviour of Room-Temperature Ionic Liquids: 1-Alkyl-3-Methylimidazolium Cations. *Phys. Chem. Chem. Phys.* **2010**, *12*, 2959−2967.

(19) Mizoshiri, M.; Nagao, T.; Mizoguchi, Y.; Yao, M. Dielectric Permittivity of Room Temperature Ionic Liquids: A Relation to the Polar and Nonpolar Domain Structures. *J. Chem. Phys.* **2010**, *132*, 164510.

(20) Turton, D. A.; Hunger, J.; Stoppa, A.; Hefter, G.; Thoman, A.; Walther, M.; Buchner, R.; Wynne, K. Dynamics of Imidazolium Ionic Liquids from a Combined Dielectric Relaxation and Optical Kerr Effect Study: Evidence for Mesoscopic Aggregation. *J. Am. Chem. Soc.* **2009**, *131*, 11140−11146.

(21) Nicolau, B. G.; Sturlaugson, A.; Fruchey, K.; Ribeiro, M. C. C.; Fayer, M. D. Room Temperature Ionic Liquid-Lithium Salt Mixtures: Optical Kerr Effect Dynamical Measurements. *J. Phys. Chem. B* **2010**, *114*, 8350−8356.

(22) Sturlaugson, A. L.; Fruchey, K. S.; Fayer, M. D. Orientational Dynamics of Room Temperature Ionic Liquid/Water Mixtures: Water-Induced Structure. *J. Phys. Chem. B* **2012**, *116*, 1777−1787.

(23) Xiao, D.; Rajian, J. R.; Cady, A.; Li, S.; Bartsch, R. A.; Quitevis, E. L. Nanostructural Organization and Anion Effects on the Temperature Dependence of the Optical Kerr Effect Spectra of Ionic Liquids. *J. Phys. Chem. B* **2007**, *111*, 4669−4677.

(24) Xiao, D.; Rajian, J. R.; Hines, L. G., Jr.; Li, S.; Bartsch, R. A.; Quitevis, E. L. Nanostructural Organization and Anion Effects in the Optical Kerr Effect Spectra of Binary Ionic Liquid Mixtures. *J. Phys. Chem. B* **2008**, *112*, 13316−13325.

(25) Yang, P.; Voth, G. A.; Xiao, D.; Hines, L. G.; Bartsch, R. a.; Quitevis, E. L. Nanostructural Organization in Carbon Disulfide/Ionic Liquid Mixtures: Molecular Dynamics Simulations and Optical Kerr Effect Spectroscopy. *J. Chem. Phys.* **2011**, *135*, 034502.

(26) Sturlaugson, A. L.; Fruchey, K. S.; Fayer, M. D. Orientational Dynamics of Room Temperature Ionic Liquid/Water Mixtures: Evidence for Water-Induced Structure and Anisotropic Cation Solvation. *J. Phys. Chem. B* **2012**, *116*, 1777−1787.

(27) Lawler, C.; Fayer, M. D. The Influence of Lithium Cations on Dynamics and Structure of Room Temperature Ionic Liquids. *J. Phys. Chem. B* **2013**, *117*, 9768−9774.

DOI: 10.1021/acs.jpcb.6b07853
J. Phys. Chem. B 2016, 120, 10350−10357

(28) Wirth, P.; Schneider, S.; Dörr, F. S1-Lifetimes of Triphenylmethane and Indigo Dyes Determined by 2-Photon-Fluorescence Technique. *Opt. Commun.* **1977**, *20*, 155−158.
(29) Giammanco, C. H.; Kramer, P. L.; Yamada, S. A.; Nishida, J.; Tamimi, A.; Fayer, M. D. Carbon Dioxide in an Ionic Liquid: Structural and Rotational Dynamics. *J. Chem. Phys.* **2016**, *144*, 104506.
(30) Kramer, P. L.; Giammanco, C. H.; Fayer, M. D. Dynamics of Water, Methanol, and Ethanol in a Room Temperature Ionic Liquid. *J. Chem. Phys.* **2015**, *142*, 212408.
(31) Tamimi, A.; Fayer, M. D. Ionic Liquid Dynamics Measured with 2D IR and IR Pump−Probe Experiments on a Linear Anion and the Influence of Potassium Cations. *J. Phys. Chem. B* **2016**, *120*, 5842−5854.
(32) Canongia Lopes, J. N. A.; Pádua, A. A. H. Nanostructural Organization in Ionic Liquids. *J. Phys. Chem. B* **2006**, *110*, 3330−3335.
(33) Tran, C. D.; Lacerda, S. H. D.; Oliveira, D. Absorption of Water by Room-Temperature Ionic Liquids: Effect of Anions on Concentration and State of Water. *Appl. Spectrosc.* **2003**, *57*, 152−157.
(34) Khupse, N. D.; Kumar, A. Delineating Solute-Solvent Interactions in Binary Mixtures of Ionic Liquids in Molecular Solvents and Preferential Solvation Approach. *J. Phys. Chem. B* **2011**, *115*, 711−718.
(35) Ries, L. A. S.; do Amaral, F. A.; Matos, K.; Martini, E. M. A.; de Souza, M. O.; de Souza, R. F. Evidence of Change in the Molecular Organization of 1-N-Butyl-3-Methylimidazolium Tetrafluoroborate Ionic Liquid Solutions with the Addition of Water. *Polyhedron* **2008**, *27*, 3287−3293.
(36) Kohlmann, C.; Greiner, L.; Leitner, W.; Wandrey, C.; Luetz, S. Ionic Liquids as Performance Additives for Electroenzymatic Syntheses. *Chem. - Eur. J.* **2009**, *15*, 11692−11700.
(37) Yu, L.; Clifford, J.; Pham, T. T.; Almaraz, E.; Perry, F., III; Caputo, G. A.; Vaden, T. D. Conductivity, Spectroscopic, and Computational Investigation of H3o+ Solvation in Ionic Liquid Bmibf4. *J. Phys. Chem. B* **2013**, *117*, 7057−7064.
(38) Xiao, D.; Hines, L. G.; Bartsch, R. A.; Quitevis, E. L. Intermolecular Vibrational Motions of Solute Molecules Confined in Nonpolar Domains of Ionic Liquids. *J. Phys. Chem. B* **2009**, *113*, 4544−4548.
(39) Blesic, M.; Lopes, J. N. C.; Pádua, A. A. H.; Shimizu, K.; Costa Gomes, M. F.; Rebelo, L. P. N. Phase Equilibria in Ionic Liquid-Aromatic Compound Mixtures, Including Benzene Fluorination Effects. *J. Phys. Chem. B* **2009**, *113*, 7631−7636.
(40) Shimomura, T.; Takamuku, T.; Yamaguchi, T. Clusters of Imidazolium-Based Ionic Liquid in Benzene Solutions. *J. Phys. Chem. B* **2011**, *115*, 8518−8527.
(41) Christensen, R. L.; Drake, R. C.; Phillips, D. Time-Resolved Fluorescence Anisotropy of Perylene. *J. Phys. Chem.* **1986**, *90*, 5960−5967.
(42) Jiang, Y.; Blanchard, G. J. Rotational Diffusion Dynamics of Perylene in N-Alkanes - Observation of a Solvent Length-Dependent Change of Boundary-Condition. *J. Phys. Chem.* **1994**, *98*, 6436−6440.
(43) Burrell, A. K.; Del Sesto, R. E.; Baker, S. N.; McCleskey, T. M.; Baker, G. A. The Large Scale Synthesis of Pure Imidazolium and Pyrrolidinium Ionic Liquids. *Green Chem.* **2007**, *9*, 449−454.
(44) Earle, M. J.; Gordon, C. M.; Plechkova, N. V.; Seddon, K. R.; Welton, T. Decolorization of Ionic Liquids for Spectroscopy. *Anal. Chem.* **2007**, *79*, 758−764.
(45) Barkley, M. D.; Kowalczyk, A. A.; Brand, L. Fluorescence Decay Studies of Anisotropic Rotations of Small Molecules. *J. Chem. Phys.* **1981**, *75*, 3581−3593.
(46) Chuang, T. J.; Eisenthal, K. B. Theory of Fluorescence Depolarization by Anisotropic Rotational Diffusion. *J. Chem. Phys.* **1972**, *57*, 5094−5097.
(47) Xu, J.; Shen, X.; Knutson, J. R. Femtosecond Fluorescence Upconversion Study of the Rotations of Perylene and Tetracene in Hexadecane. *J. Phys. Chem. A* **2003**, *107*, 8383−8387.
(48) Lawler, C.; Fayer, M. D. Proton Transfer in Ionic and Neutral Reverse Micelles. *J. Phys. Chem. B* **2015**, *119*, 6024−6034.
(49) Brocklehurst, B.; Young, R. N. Rotation of Aromatic Hydrocarbons in Viscous Alkanes. 1. Methylcyclohexane. *J. Phys. Chem. A* **1999**, *103*, 3809−3817.
(50) Lipari, G.; Szabo, A. Effect of Librational Motion on Fluorescence Depolarization and Nuclear Magnetic-Resonance Relaxation in Macromolecules and Membranes. *Biophys. J.* **1980**, *30*, 489−506.
(51) Wang, C. C.; Pecora, R. Time-Correlation Functions for Restricted Rotational Diffusion. *J. Chem. Phys.* **1980**, *72*, 5333−5340.
(52) Youngren, G. K.; Acrivos, A. Rotational Friction Coefficients for Ellipsoids and Chemical Molecules with the Slip Boundary Condition. *J. Chem. Phys.* **1975**, *63*, 3846−3848.
(53) Sension, R. J.; Hochstrasser, R. M. Comment On: Rotational Friction Coefficients for Ellipsoids and Chemical Molecules with Slip Boundary Conditions. *J. Chem. Phys.* **1993**, *98*, 2490−2490.
(54) Moreno, M.; Castiglione, F.; Mele, A.; Pasqui, C.; Raos, G. Interaction of Water with the Model Ionic Liquid Bmim BF4: Molecular Dynamics Simulations and Comparison with NMR Data. *J. Phys. Chem. B* **2008**, *112*, 7826−7836.
(55) Feng, S.; Voth, G. A. Molecular Dynamics Simulations of Imidazolium-Based Ionic Liquid/Water Mixtures: Alkyl Side Chain Length and Anion Effects. *Fluid Phase Equilib.* **2010**, *294*, 148−156.
(56) Sturlaugson, A. L.; Fruchey, K. S.; Lynch, S. R.; Aragón, S. R.; Fayer, M. D. Orientational and Translational Dynamics of Polyether/Water Solutionsadam L. Sturlaugson, Kendall S. Fruchey, Stephen R. Lynch, Sergio R. Aragón, and M. D. Fayer. *J. Phys. Chem. B* **2010**, *114*, 5350−5358.
(57) Cang, H.; Li, J.; Fayer, M. D. Orientational Dynamics of the Ionic Organic Liquid 1-Ethyl-3-Methylimidazolium Nitrate. *J. Chem. Phys.* **2003**, *119*, 13017−13023.
(58) Götze, W.; Sperl, M. Nearly Logarithmic Decay of Correlations in Glass-Forming Liquids. *Phys. Rev. Lett.* **2004**, *92*, 105701.

DOI: 10.1021/acs.jpcb.6b07853
J. Phys. Chem. B 2016, 120, 10350−10357